Pattern Recognition Letters 33 (2012) 951–961

Contents lists available at SciVerse ScienceDirect

Pattern Recognition Letters

journal homepage: www.elsevier.com/locate/patrec

Prostate cancer grading: Gland segmentation and structural features ☆

Kien Nguyen [a], Bikash Sabata [b], Anil K. Jain [a,*,1]

[a] Michigan State University, East Lansing, MI 48824, USA
[b] Ventana Medical Systems, Inc., 919 Hermosa Ct, Sunnyvale, CA 94085, USA

ARTICLE INFO

Article history:
Available online 10 October 2011

Keywords:
Prostate cancer
Benign
Carcinoma
Gleason grading system
Gland segmentation
Nuclei

ABSTRACT

In this paper, we introduce a novel approach to grade prostate malignancy using digitized histopathological specimens of the prostate tissue. Most of the approaches proposed in the literature to address this problem utilize various textural features computed from the prostate tissue image. Our approach differs in that we only focus on the tissue structure and the well-known Gleason grading system specification. The color space representing the tissue image is investigated and basic components of the prostate tissue are detected. The components and their structural relationship constitute a complete gland region. Tissue structural features extracted from gland morphology are used to classify a tissue pattern into three major categories: benign, grade 3 carcinoma and grade 4 carcinoma. Our experiments show that the proposed method outperforms a texture-based method in the three-class classification problem and most of the two-class classification problems except for the grade 3 vs grade 4 classification. Based on these results, we propose a hierarchical (binary) classification scheme which utilizes the two methods and obtains 85.6% accuracy in classifying an input tissue pattern into one of the three classes.

1. Introduction

Prostate cancer is a type of cancer that occurs in men's reproductive system. In the United States, it is the second most prevalent cancer in men and it is also one of the leading causes of death by cancer (in 2006, prostate cancer developed in 203,415 men and killed 28,372 men) (US Cancer Statistics Working Group, 2010). Prostate cancer grows slowly with very few symptoms; it develops mostly in men over the age of fifty. Prostate cancer is considered serious because of the threat of its invasion (metastasis) into other organs such as bones, bladder and rectum. The prognosis involves a screening (such as digital rectal examination or prostate-specific antigen (PSA) test (Catalona et al., 1991)) and, if necessary, a follow-up prostate biopsy. After an unsuspected cancer is revealed via the screening, a biopsy is used to confirm it. A CT scan or a bone scan can be employed additionally to determine the spread of the cancer.

The biopsy is conducted by a radiologist or a urologist. First, a prostate tissue sample is removed from the patient for inspection under a microscope. A grade is then reported for the tumor derived from the tissue. The most widely used grading method is Gleason grading (Gleason, 1977, 1992), which assigns a numerical grade from 2 to 10 to the tumor. The grade is based solely on structural features of the tissue and excludes cytological features (Mason, 1964). In this grading method, a pathologist finds the most predominant and the second most predominant histological carcinoma patterns in the tissue, assigns each of them a score (from 1 to 5) and adds the two scores together to obtain the final Gleason grade (2 to 10) for the tissue. The grade of each carcinoma pattern is based on its differentiation (how much of its structure resembles a normal pattern structure). A grade 1 carcinoma pattern is very well differentiated and a grade 5 carcinoma pattern is very poorly differentiated. The change in tissue structure is good evidence for this differentiation. More specifically, in Gleason grades 1 and 2, most of the glands appear as single units, separated from each other, densely packed, and there is no infiltration of these glands into benign tissue areas (this is very close to the structure of a normal tissue). Gleason Grade 3, the most common case of carcinoma, is characterized by the invasion of small glands into the muscle (stroma). In Gleason grade 4, glands are fused with each other and poorly defined; glands are not well-separated by stroma as in lower grades. Finally, in Gleason grade 5, there is no evidence of the formation of gland units in the pattern. A visual summarization of these five grades can be found in Fig. 1. Pathologists face a number of difficulties in manually diagnosing prostate cancer, i.e. to look at the prostate tissue under a microscope is tedious and time-consuming. Moreover, the diagnostic accuracy depends on the personal skill and experience of a pathologist. These problems motivate the research and development for automating the diagnosis and prognosis processes.

☆ A preliminary version of this paper appeared in the Proceedings of the 20th ICPR, Istanbul, August 2010.

* Corresponding author. Tel.: +1 517 355 9282.
E-mail addresses: nguye231@msu.edu (K. Nguyen), bikash.sabata@bioimagene.com (B. Sabata), jain@cse.msu.edu (A.K. Jain).
[1] Also affiliated to Department of Brain & Cognitive Engineering, Korea University, Seoul.

0167-8655/$ - see front matter © 2011 Elsevier B.V. All rights reserved.
doi:10.1016/j.patrec.2011.10.001

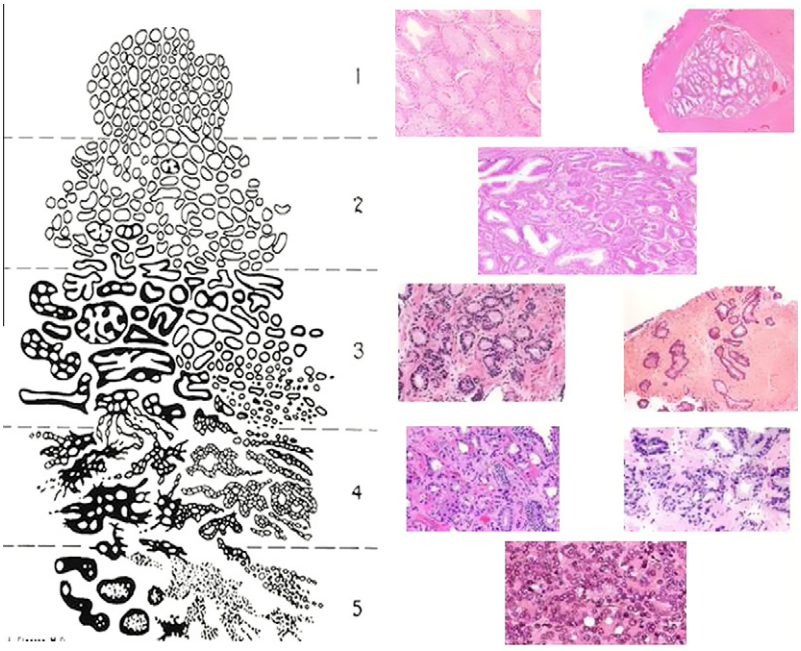

Fig. 1. Five grades of the Gleason grading applied to histological patterns of the prostate tissue.

In most digital pathology studies on computer-aided prognosis for prostate cancer, textural features of the image and structural features of the tissue have been widely used. Diamond et al. (2004) used co-occurrence texture features (Haralick et al., 1973) to classify each 100 × 100 sub-region in a tissue image into either stroma or prostatic carcinoma. In addition, lumen area was used to discriminate benign tissue from the other two classes. They reported 79.3% accuracy when evaluating the algorithm on sub-regions of 8 tissue images (40× magnification). A cancer vs non-cancer classification problem which used 594 features including first-order statistics (average, median, standard deviation), co-occurrence and wavelet features was addressed in Doyle et al. (2006). The algorithm was implemented at three different scales of the image. At each scale, a Bayes classifier was designed for each feature individually, resulting in 594 base learners for AdaBoost. The reported accuracy was 88% on a dataset of 22 images (40× magnification). In Tai et al. (2010), fractal dimension features were calculated for the tissue image and the low frequency sub-bands of the image to discriminate the textural discrepancy between low grade and high grade carcinoma. By using an SVM classifier with leave-one-out technique, the method achieved 86.3% accuracy for the classification of 1,000 prostatic biopsy images into normal, grade 3, grade 4 and grade 5 classes. A multiwavelet transform was used as the main texture analysis tool in Khouzani and Zadeh (2003). The features used for classification included entropy and energy derived from the multiwavelet coefficients of the image. Ten different types of multiwavelet were evaluated on a dataset of 100 prostate sample images (100× magnification) of grades 2, 3, 4 and 5, resulting in the best accuracy of 97%. In another study, Tabesh et al. (2007) employed both global features of the entire image and local features of every object in the image. Global features included color histogram, fractal features, texture and morphometry of the image. Local features were computed for histological objects such as nuclei, stroma and lumen, which were extracted by the MAGIC system (Teverovskiy et al., 2004). They achieved 96.7% accuracy for tumor-nontumor classification (fivefold cross validation with 367 images) and 81% accuracy for low grade-high grade classification (fivefold cross validation with 268 images). All images were at 20× magnification. A segmentation-based method was presented in Naik et al. (2008). They first used a Bayesian classifier to place every pixel in the image into one of the three classes: lumen, nuclei and cytoplasm based on its color. Lumen pixels were first grouped together and lumen objects were then identified as the groups satisfying the gland size constraint. The inner boundary of the glands, which is the border of the nuclei and the cytoplasm surrounding the lumen, was detected using a level set formulation. Eight shape features for each of the lumen and the gland inner boundary were calculated. A tissue was classified into benign, a grade 3 carcinoma or a grade 4 carcinoma via an SVM classifier. However, by using a dataset that included 44 images at 40× magnification, they only reported results of two-class classifications: 86.35% accuracy when classifying grade 3 carcinoma and benign, 92.9% accuracy when classifying grade 4 carcinoma and benign, and 95.19% accuracy when classifying grade 3 carcinoma and grade 4 carcinoma. Three-class classification result was not reported. Table 1 summarizes the related studies discussed in this section.

In this study, we present a segmentation-based method to classify a tissue pattern into three common cases based on Gleason grading: benign, grade 3 and grade 4 carcinoma. However, unlike Naik et al. (2008), we incorporate nucleus and blue mucin information into the glandular structures which are used for the classification. It is apparent from the tissue pattern image that nucleus distribution changes remarkably among various cancer stages (in benign tissue, nuclei form a ring on the gland boundary and scatter in other areas (Fig. 8(a)) while in grade 4 carcinoma, nuclei distribute more uniformly over the glandular regions (Fig. 8(c))) and mucin appears commonly in cancerous glands (Fig. 8(b)). While a gland region in Naik et al. (2008) solely consists of lumen and internal cytoplasm region, our segmentation procedure leads to complete glands which include their nucleus boundaries. Moreover, the structural features extracted in our method do not require a very high magnification (like 40× in Naik et al., 2008) to achieve state of the art classification results. The proposed algorithm is designed to work for images created from the Hematoxylin and Eosin (H&E) staining method (Kiernan, 2001). The outline of the methodology is delineated in the flowchart of Fig. 2. Given an input tissue pattern, we first segment glands from the stroma area (this comprises steps 1, 2, 3, 4 in the flowchart). Once gland regions